15B.6 THE EFFECTS OF HORIZONTAL GRID SPACING AND VERTICAL RESOLUTION ON TAMDAR DATA ASSIMILATION IN SHORT-RANGE MESOSCALE FORECASTS

Neil Jacobs[1*], Peter Childs[1], Meredith Croke[1], and Yubao Liu[2]

[1]AirDat LLC, Morrisville, NC 27560
[2]National Center for Atmospheric Research, Boulder, CO 80307

1. INTRODUCTION AND MOTIVATION

Lower and middle-tropospheric observations are disproportionately sparse, both temporally and geographically, when compared to surface observations. The unsubstantial density of observations is likely one of the largest limiting factors in numerical weather prediction.

Atmospheric measurements performed by the Tropospheric Airborne Meteorological Data Reporting (TAMDAR) sensor of humidity, pressure, temperature, winds aloft, icing, and turbulence, along with the corresponding location, time, and altitude from built-in GPS are relayed via satellite in real-time to a ground-based network operations center.

Since December 2004, the TAMDAR sensors have been operating on a fleet of 63 Saab 340s operated by Mesaba Airlines in the Great Lakes region as a part of the NASA-sponsored Great Lakes Fleet Experiment (GLFE). Equipage of sensors on additional aircraft across the continental US and Alaska is currently underway. More than 800 soundings are generated from 400 flights to 75 regional airports during a 24-h period. Upon completion of the 2008 installation, more than 5000 daily sounding will be produced.

A study of the impact of the TAMDAR data on mesoscale NWP is conducted using a mesoscale model, which employs various assimilation techniques and the available TAMDAR data. The first study reconducts the sensitivity experiment from Jacobs et al. (2007) using RAOB observations as verification instead of the North American Regional Reanalysis (NARR). The motivation for changing the verification method is two-fold. First, there was an inherent incestuous relationship between the NARR and the models being tested in that the forecast model employs boundary conditions provided by the same code which assimilates observations for construction of the NARR. This lead to a significantly better correlation, including the control runs, between the forecast output and the NARR (truth). An example of this improved correlation is shown in Fig. 1, where the forecasted RH is verified against NARR (r=0.75) and a RAOB (r=0.56). There are likely many reasons for such aliasing, and to avoid them, RAOB data was considered truth in this study. Secondly, ongoing studies at NOAA/ERSL/GSD use RAOBs to evaluate forecast skill of the Rapid Update Cycle (RUC; Benjamin et al. 2007). For interest in comparing forecast skill of RUC, WRF and MM5, we are implementing this more consistent methodology.

As in the original study, six parallel 12-h simulations, where the three experimental (control) runs include (withhold) TAMDAR data, are performed, with one of the three pair of experimental and control simulations having 36 σ-levels, while the other two pair of experimental and control simulations have 48 σ-levels. One of the 48-σ-level pairs has a single domain of 10-km grid spacing, while the other two pair have a 36-km outer domain which feeds a 12-km inner domain.

The objectives of this study are to (i) optimize impacts that TAMDAR data may have on the forecast system by increasing the horizontal distribution of vertical atmospheric profiles during initialization, and (ii) to isolate the effects of data assimilation at a higher horizontal and vertical resolution with respect to temperature and relative humidity forecast variables.

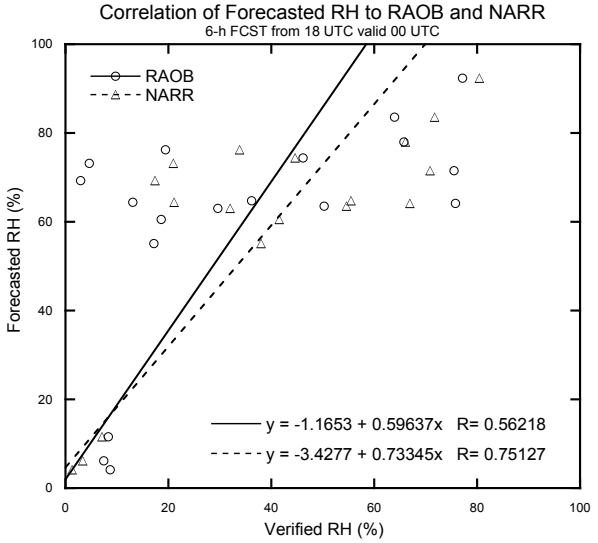

Fig. 1. Forecasted RH verification correlation using NARR (dashed) and a RAOB (solid).

2. METHODOLOGY AND MODEL CONFIGURATION

Following the methodology of the previous study, there are six parallel model runs in this study (Table 1). The AirDat-standard run (AD) features an outer domain of 36-km grid spacing and a two-way nested 12-km inner domain. The AD run has 36 σ-levels and assimilates the TAMDAR data. The AirNot-standard run (AN) has an identical model configuration except AN does not include TAMDAR data. The AirDat-2 (AD2) and AirNot-2 (AN2)

[*]*Corresponding author address*: Neil A. Jacobs, AirDat, LLC, 2400 Perimeter Park Dr. Suite 100, Morrisville, NC 27560. Email: njacobs@airdat.com

runs have an identical nested-domain structure to both the AD and AN runs; however, 12 additional σ-levels have been added in both AD2 and AN2 for a total of 48 levels. As in AD and AN, the only difference between AD2 and AN2 is that AD2 assimilates TAMDAR data, while AN2 does not. The majority of the additional σ-levels for AD2 and AN2 are added in the lowest 3 km, or between the 1000 and 700-hPa pressure-levels. This spacing was chosen to best utilize the observation density provided by the TAMDAR data. The final two parallel simulations are the AirDat-10 (AD10) and the AirNot-10 (AN10). These two runs have only one domain of 10-km grid spacing. This domain has the same latitude and longitude dimensions as the outer domain of the previously discussed runs. Both the AD10 and AN10 runs have 48 σ-levels, which are identically spaced to those in the AD2 and AN2 runs.

RUN	OUTER DOMAIN	INNER DOMAIN	LEVELS	TAMDAR
AD	36 KM	12 km	36	Yes
AN	36 KM	12 km	36	No
AD2	36 KM	12 km	48	Yes
AN2	36 KM	12 km	48	No
AD10	10 KM	None	48	Yes
AN10	10 KM	None	48	No

Table 1. The six different parallel model runs in this study

There are multiple angles to this study. First, comparisons are drawn between the like-runs (e.g., AD to AN, AD2 to AN2, etc.) to ascertain any TAMDAR-related impacts. Additionally, comparisons are drawn between AD, AD2, and AD10, with the AN runs as controls, to quantify the effects of increased vertical resolution on the utilization of TAMDAR data. Finally, comparisons are drawn between the AD and AD2 runs to the AD10 run to quantify any change in forecast skill as a function of finer horizontal radial influence during the observation assimilation stage. Part of the motivation for this test stems from the tendency for dry air that is observed from airplanes that circumnavigate convective systems to reduce the moisture analysis by having a nudging radius much larger than the distance of the plane from the storm. The hypothesized solution simply requires a finer outer mesh to allow for a reduced radius of influence.

The study covers the entire month of May 2006. The MM5 simulations were initialized at 1800 UTC for all model runs. All simulations were initialized with identical analysis fields provided by the NCAR/AirDat RT-FDDA-MM5. The NCAR/AirDat RT-FDDA system is built around the Fifth Generation of the Penn State/National Center for Atmospheric Research (PSU/NCAR) Mesoscale Model (MM5, Dudhia 1993; Grell et al. 1994). The outer domain of the RT-FDDA-MM5 has a 100 x 97 grid spacing of 36 km, and is centered over the Great Lakes region (Fig. 2). A continuous data ingestion system using Newtonian relaxation is utilized during an analysis period to generate balanced 4-D analyses. This method greatly reduces the time and errors associated with typical model spin-up (Stauffer and Seaman 1994; Cram et al. 2001; and Liu et al. 2002). The NCAR/AirDat RT-FDDA is run on a 3-h cycle with cycle times occurring at 23Z, 2Z, 5Z, 8Z, 11Z, 14Z, 17Z, and 20Z. For this study, the 1-h output from the 1700 UTC RT-FDDA cycle, valid 1800 UTC, were used as first-guess fields. These files include 1 hour of additional 4DDA nudging; however, they do not include TAMDAR data (i.e., AIRNOT cycles). After the first-guess field is generated, it is then passed through a 3DVAR-style technique to assimilate additional observations and construct the analysis from which each MM5 simulation is initialized. All of the additional observations are identical for all runs with the exception of the TAMDAR data, which is only assimilated by the AD runs using this 3DVAR approach. Ongoing studies at AirDat (presented in section 4) and NCAR suggest that significant improvements in forecast skill are realized when using a true 4DVAR assimilation technique; however, for consistency with Jacobs et al. (2007), 3DVAR is employed.

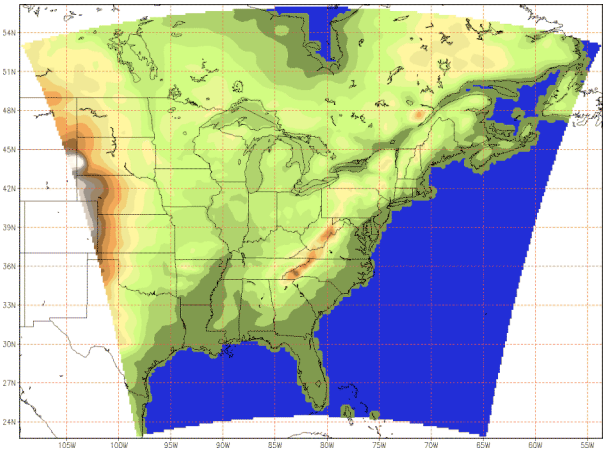

Fig. 2. The Lambert conformal grid for the outer domain of all the simulations.

The MM5 was employed as a means to ascertain optimal combinations and settings for various ingestion, weighting, resolution, and parameterization options. Extensive testing of various parameterizations has been performed to optimize the impact of TAMDAR data (Jacobs and Liu 2006; Jacobs et al. 2006). Those studies suggest that the Kain-Fritsch (KF) cumulus parameterization (CP) is better suited for 20 to 30-km grid spacing, while the Grell CP is better suited for 10-km spacing, and are consistent with findings from Kain and Fritsch (1993). Kain-Fritsch, which generates more convection, may be acceptable if only using the 36-km domain, but when that domain is used as boundary conditions for a finer nested domain such as 12-km, too much convective feedback may occur. Additionally, some CP schemes are better for summer and tropical convection, and some are better for winter mid-latitude convection. Grell tends to handle thunderstorms much better, while KF handles winter frontal systems better (Mahoney and Lackmann 2005). Based on these findings, as well as the season of the study, the Grell cumulus parameterization was chosen for its handling of

convective precipitation at smaller grid scales. The MRF planetary boundary layer scheme, as well as the Mixed-phase (Reisner-1) microphysics were also chosen to be consistent with the analysis field generation methods. All simulations were integrated for 12 hours; however, only the forecast-hour 6 (i.e., 0000 UTC for the 1800 UTC run) was used for verification purposes. The original Jacobs et al. (2007) study also compared 0600 UTC runs, but those are not included here, as the largest TAMDAR-related impact is expected between 1400 and 1800 UTC based on flight times.

To verify the forecast output, model-generated soundings were produced at three locations: Minneapolis/St. Paul, MN (KMPX; 44.8489 N, 93.5656 W; Elev: 946'), Detroit/Pontiac, MI (KDTX; 42.6997 N, 83.4717 W; Elev: 1072'), and Green Bay, WI (KGRB; 44.4983 N, 88.1114 W; Elev: 682'). The motivation for choosing the locations of KMPX and KDTX was based on data density. Both airport locations are regional hubs for Mesaba Airlines. It is assumed that the largest possible data-density-related impacts will be realized in the vicinity of these hubs. KGRB was also included as a 3rd non-hub location because it is located between the other two, and quite often is in line with direct flight paths between KMPX and KDTX.

In Jacobs et al. (2007), the model-generated soundings were compared to soundings taken from the North American Regional Reanalysis (NARR), which was obtained from NCDC's NOMADS[1] archive (Kalnay et al. 1990; Mesinger et al. 2006). The NARR/Regional Climate Data Assimilation System (R-CDAS) is an extension of the NCEP Global Reanalysis (GR), which is run over the CONUS. The NARR uses the high resolution NCEP Eta Model (32km/45 layer) together with the Regional Data Assimilation System (RDAS). For this study, the model-generated soundings were compared to RAOB observations. The RH value is obtained from the RAOB temperature and dewpoint using the calculation outlined in Bolton (1980).

The forecast bias is simply defined as the 6-hour forecast value (X) minus the observed value (θ). In the case of the 1800 UTC simulations, differences are calculated at 0000 UTC. The forecast RMS error is defined as

$$RMSE(X) = \left(\frac{1}{n} \sum_{n=1}^{n} \left(X - \overline{X} \right)^2 + \left(X - \theta \right)^2 \right)^{\frac{1}{2}}, \qquad (1)$$

where n is the number of compared values. Since there is one run a day, for this case it is equal to the number of days. A percent reduction in error is seen as a percentage increase in forecast skill. This percent improvement is defined as

$$\%IMP = -\frac{\alpha - \beta}{\beta} \times 100, \qquad (2)$$

where simulation α is compared to simulation β, and appears contextually below as α versus β (Brooks and Doswell 1996).

3. SENSITIVITY TO σ-LEVEL DENSITY AND HORIZONTAL GRID SPACING

It should be noted that all of the plots below correspond to the 0000 UTC comparison. The 0000 UTC time historically shows a larger difference because (i) there are more flights between 1400 and 2200 UTC, and (ii) the lower-troposphere is less stable. The figures presented here are plotted from the average statistics derived from the three locations of verification. There is noticeably less divergence between the model runs at the KDTX location. This could possibly be related to fewer flights, as well as less thermal variability from Great Lakes-enhanced boundary layer moisture content.

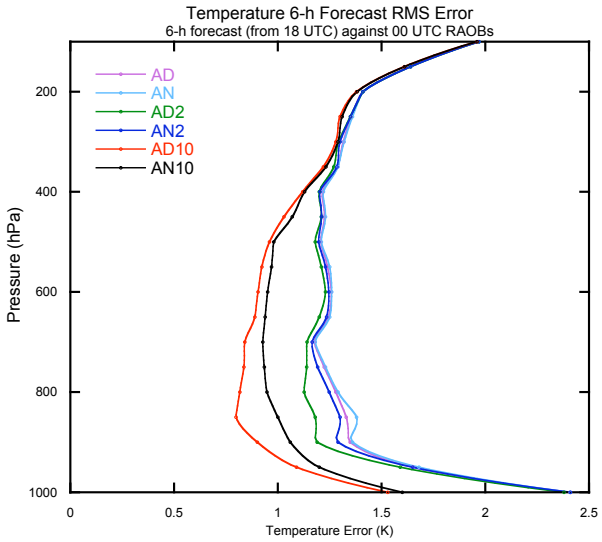

Fig. 3. Vertical profile of 6-h temperature RMS error verified against 00 UTC RAOBs for May 2006. Average of the three locations KMPX, KDTX, KGRB.

The 6-h temperature forecast error shown in Fig. 3 appears to be greater in magnitude above 300 hPa; however, it is assumed to be unrelated to the TAMDAR data and grid variations since similar trends are seen for all simulations. Divergence between the simulations begins to occur around 400 hPa. Between 400 and 800 hPa, the error in the runs diverge further, but in general, the error magnitude does not change. The AN/AD and AN2/AD2 runs have an average error around 1.4 K, while the AN10/AD10 runs have errors around 1 K. It is evident from these differences that a finer outer grid during the data assimilation phase improves the forecast skill. Below 900 hPa, the error increases, but appears to increase at more than twice the rate in the 4 runs with larger grid spacing. It is assumed that this is likely from the large variability of the surface temperature. Similar trends are also seen above 200 hPa, which could either be from RAOB drift or boundary conditions. Below 650

[1] http://nomads.ncdc.noaa.gov/

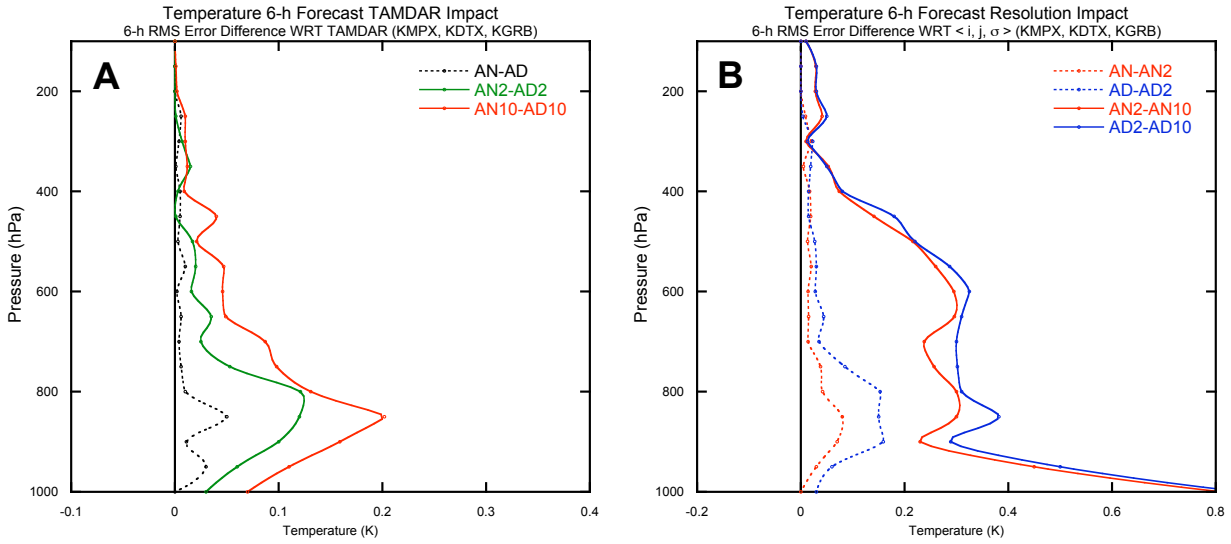

Fig. 4. Vertical profile of 6-h temperature RMS error difference (AirNot-AirDat) as a function of TAMDAR impact (A), and as a function of model resolution (B).

hPa, both AD2 and AD10 show a noticeable decrease in error over AN and AN2, as well as even the AD run.

The method for quantifying forecast skill is given by (2). The improvement as a function of TAMDAR data for temperature is shown in Fig. 4A. Minor positive impact is seen for the AD run over the AN run (black dashed), while the largest improvement noted is between AD10 and AN10. The positive impact of TAMDAR data in the AD2 run over the AN2 was not as significant, but closer to the AD10 improvement, which suggests vertical resolution plays a role in forecast skill with respect to TAMDAR assimilation. The largest reduction in error, approximately 0.2 K, occurs near the 850 hPa level. As in most TAMDAR impact studies, this is typical and expected.

The improvement in temperature forecast skill as a function of grid spacing and vertical resolution is shown in Fig. 4B. It is evident that the increase in vertical resolution between AN and AN2 made only a very slight positive contribution. Whereas, the increase in horizontal resolution results in significant improvement. In both cases, the TAMDAR-included runs (blue) show greater forecast skill, which suggests that observation-specific assimilation protocol is dependent on model resolution, and likely increases as a function of data density. The increase in skill, which peaks for both near 850 hPa, is likely a function of the additional σ-levels being evenly spaced between the previous lower and middle-tropospheric levels.

A vertical profile of the 6-h relative humidity forecast error (%), averaged for the entire month of May 2006, is shown in Fig. 5. All simulations follow a similar trend above 200 hPa. Between 200 and 500 hPa, significant divergence between the two 10-km simulations and the other runs appears. The error in both AD10 and AN10 ranges from 15 to 20% above 500 hPa, and improves to 10 to 15% below 800 hPa. The decrease in error seen

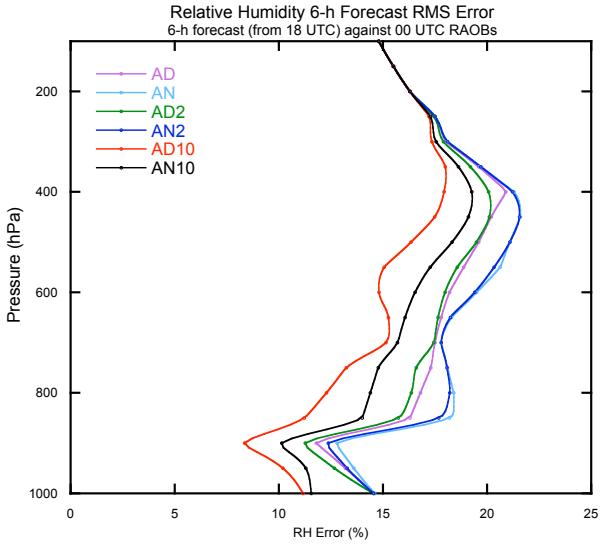

Fig. 5. Vertical profile of 6-h relative humidity RMS error verified against 00 UTC RAOBs for May 2006. Average of the three locations KMPX, KDTX, KGRB.

around the 700 hPa level for the TAMDAR-excluded runs was somewhat expected, as that is a mandatory level, and typically has a large amount of observations. Interestingly, at that same level, the TAMDAR-included runs show an increase in error, albeit less than the respective control runs. One possible explanation for this is the interaction of the TAMDAR observations with the non-TAMDAR observations during the weighting phase of the assimilation step. AD10, and to a lesser degree AN10, outperform the other runs throughout the profile. The lowest error (8.5%) was recorded by the AD10 run on the 900 hPa level, which was the same level for the AN10 run lowest error of 10.1%. The errors

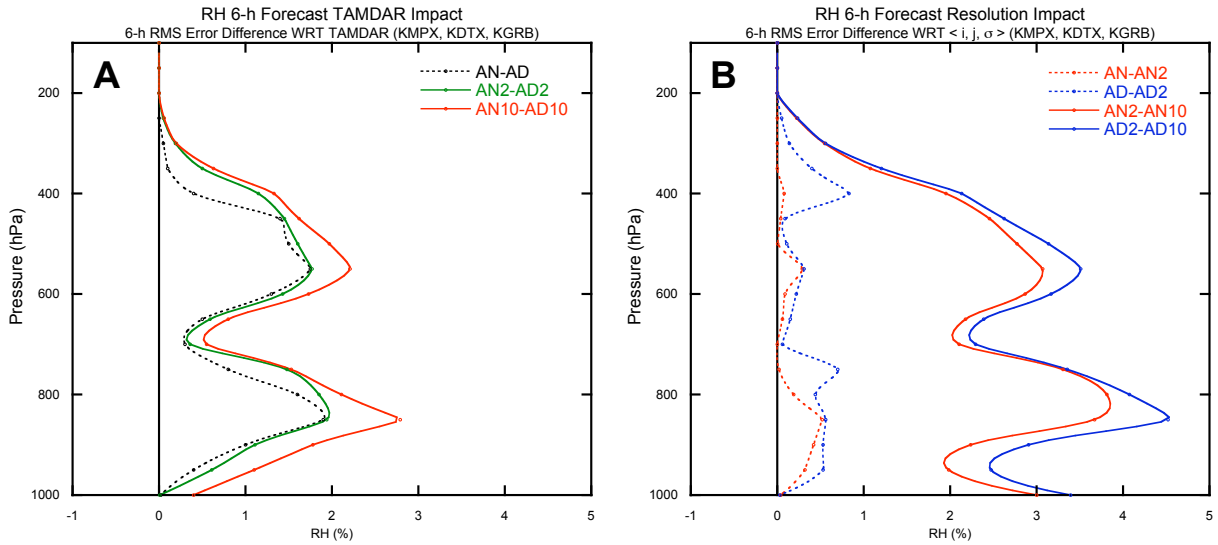

Fig. 6. Vertical profile of 6-h relative humidity RMS error difference (AirNot-AirDat) as a function of TAMDAR impact (A), and as a function of model resolution (B).

at 850 hPa, where the largest TAMDAR impact is typically seen, are 11.3 and 12.4% for the AD10 and AN10 runs, respectively. The lowest errors seen in the AD2 and AN2 runs were also on the 900-hPa level, and are 11.2 and 14.0%, respectively.

The most notable improvement as a function of TAMDAR data appears to be linked to the utilization of RH observations in the AD10 simulation (Fig. 6A). A reduction in error (> 2%) is seen between AD10 and AN10, which reaches a maximum of 2.8% at the 850 hPa level. The other two comparisons show similar trends, but to a lesser magnitude. There is a second peak reduction in error between the 550 and 450 hPa levels. This is likely caused by the increased skill of the model around the 700 hPa level, as a function of non-TAMDAR observation density.

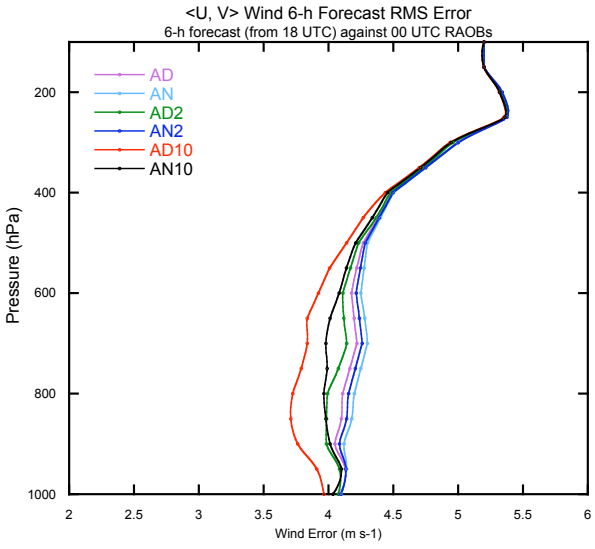

Fig. 7. Vertical profile of 6-h wind RMS error verified against 00 UTC RAOBs for May 2006. Average of the three locations KMPX, KDTX, KGRB.

A similar trend of slight improvement between AN/AD and AN2/AD2 is seen for RH (Fig. 6B). As seen with temperature, the same decrease in horizontal grid spacing produced significant differences between the other simulations. The improvement in forecast skill from the addition of TAMDAR on the 850 hPa level was on the order of 10-12% for both the AD and AD2 runs. The improvement in forecast skill from the addition of TAMDAR in the AD10 run on the 850 hPa level was 20%. The RH forecast skill as a function of grid spacing increased 28.7% from the AD2 to AD10 run.

The vertical profile of the 6-h wind forecast error (m s^{-1}) is shown in Fig. 7. An increase in the wind error is seen near the top of the profile. Since all of the simulations align while showing identical trends in this region, it is assumed that this bias is either MM5 code-related or a function of the boundary conditions. The important focus of the study deals with the differences between the runs, more than the error magnitude, within the lower and middle troposphere. The AD10 simulation clearly outperforms the other runs throughout the vertical profile. The error from 1000 to 400 hPa is steady around 4 m s^{-1}. The addition of TAMDAR data decreased the error by about 0.27 m s^{-1} on the 850 hPa level (Fig. 8A). Improvements of approximately 0.1 m s^{-1} are seen for most of the lower and middle troposphere. The error difference with respect to model resolution largely favored the 10-km runs between 450 and 850 hPa (Fig. 8B).

4. RECENT MODEL TESTING

Recently, AirDat has been running several different models and various configurations of those models to test parameterizations and assimilation methods. Some very initial testing suggests that the 3DVAR WRF-ARW, using identical data for initialization, has an edge over the 3DVAR MM5 counterpart. Some quick comparisons were done for the 12-h forecasted 850-hPa fields against

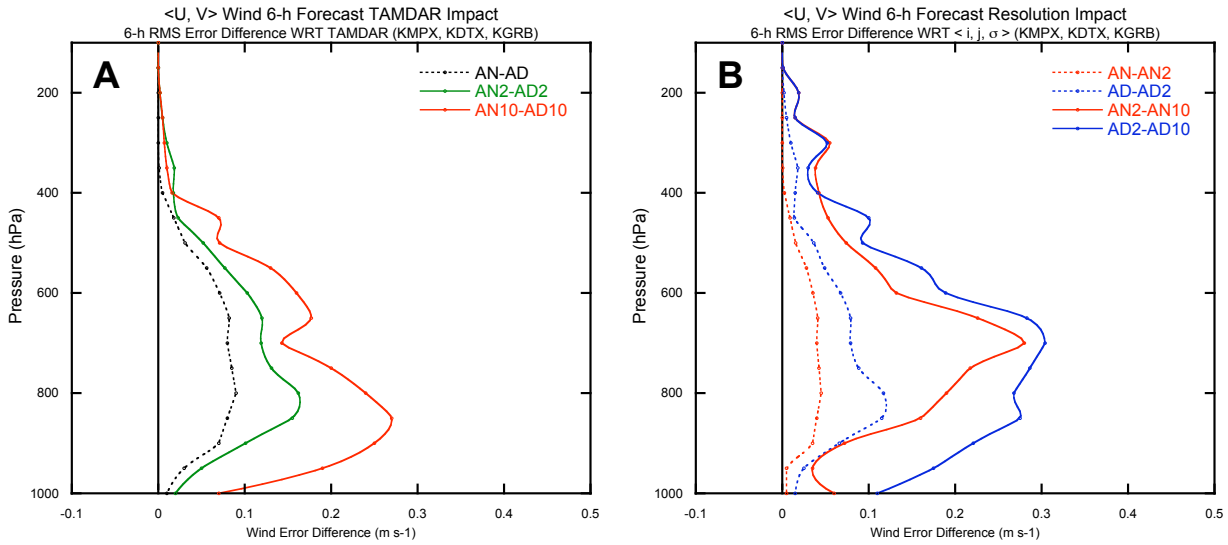

Fig. 8. Vertical profile of 6-h wind RMS error difference (AirNot-AirDat) as a function of TAMDAR impact (A), and as a function of model resolution (B).

the operational GDAS analysis, as NARR was not available at the time. Not surprisingly, the 4DVAR MM5 (RT-FDDA) performed the best with an explained variance of 83% (Fig. 9), 8% better than 3DVAR WRF (Fig. 10) and 17% better than the nearly-identically configured 3DVAR MM5 (Fig. 11).

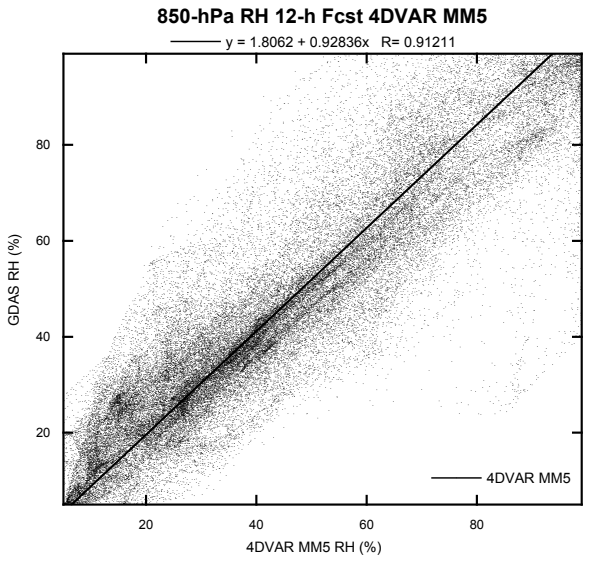

Fig. 9. 850-hPa RH verification against operational GDAS for 4DVAR (RT-FDDA) MM5 valid 00 UTC 11 Jan 2008.

The comparisons between WRF-ARW and MM5 suggest that the WRF-ARW has a slight edge outside of the data assimilation. However, this is just for one case, and several months of monitoring need to be completed before this can be considered a trend. The comparison between the 4DVAR MM5 (RT-FDDA) suggests that this assimilation method is significantly better. Again, months of testing are needed to quantify the trend. It should be mentioned that all of these runs include TAMDAR data, and the 4DVAR assimilation method assimilates all available observations in this style, not just TAMDAR. AirDat will also be adding a 4DVAR version of WRF in the near future. Additional results will be presented at the conference.

5. CONCLUSIONS

The degree of forecast skill improvement presented here is seen as a best-case result with the current level of model optimization and data quality because the verification locations are Mesaba Airlines hubs, which naturally hosts the greatest density of observations. It is assumed that additional regions surrounding (and downstream) of future fleet hubs will likely realize similar improvements

Results suggest that the addition of TAMDAR data improves all three experimental simulations for key model variables, albeit to various degrees. In general, increasing the number of σ-levels from 36 to 48 results in better utilization of the higher resolution TAMDAR data.

The most notable improvements, when increasing the number of model σ-levels, were found to occur in the vicinity of 850 hPa. This peak is likely a result of the balance between the increase in TAMDAR observations and the increase in expected model error (i.e., seen in the control runs) when approaching the surface layer from the middle-troposphere.

Changing the outer domain grid spacing from 36 km to 10 km reduces the bias and error for both the experimental (AD10) and the control (AN10); however, the magnitude of reduction is greater in AD10. This is likely because all of the non-TAMDAR observations assimilated into the first-guess fields of both runs improved the respective analysis fields. The additional

reduction in error magnitude seen in AD10 is attributed to the TAMDAR data (the only difference between AD10 and AN10).

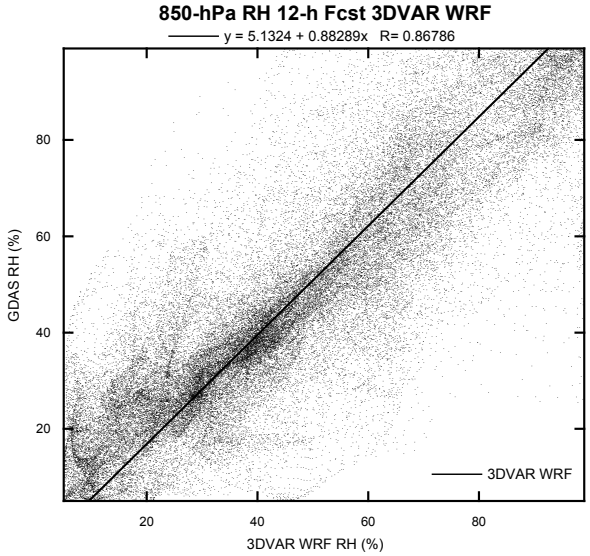

Fig. 10. 850-hPa RH verification against operational GDAS for 3DVAR WRF-ARW valid 00 UTC 11 Jan 2008.

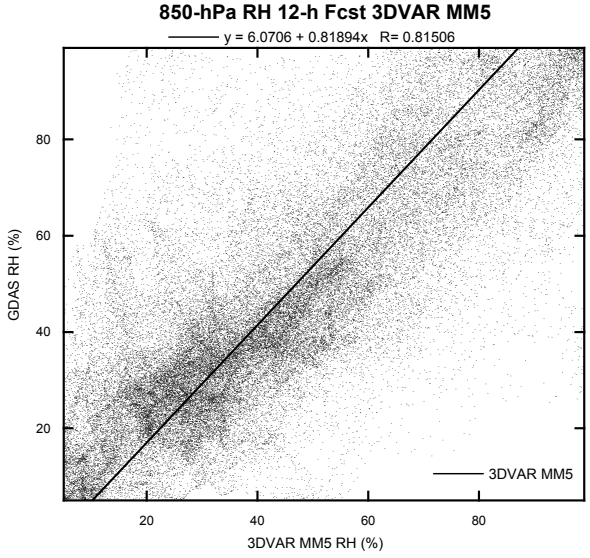

Fig. 11. 850-hPa RH verification against operational GDAS for 3DVAR MM5 valid 00 UTC 11 Jan 2008.

There are a few possibilities that may have influenced this outcome since the observations are only assimilated into the outermost grid. With a larger grid spacing, the error statistics of observations which are interpolated to identical (i, j, k) grid space can negatively influence the impact of redundant observations. The probability of this occurrence is reduced when assimilating data into a finer horizontal grid because the frequency of interpolating to identical (i, j, k)-space is reduced. The former appears to be a less problematic choice when using a background error-covariance matrix based on a larger grid in conjunction with TAMDAR data, which posses greater variability in wind-field errors when compared to the lower mass-field errors. Further cost function analysis is required to avoid pitfalls outlined by Xie et al. (2002).

In the original Jacobs et al. (2007) study, statistics from the non-10 km runs were obtained from the inner nested 12-km grid. It was later discovered that the nestdown step in the model was further forcing the inner grid towards boundary conditions, which were obtained from the same code as that which assimilates the NARR. The previous method of NARR verification was subject to a bias favoring the models in general (i.e., the controls as well), but even more for the nested inner grids. Verification in this study takes place on the 36 km grid, and is likely the reason for the difference in results for the model-to-model skill delta. The overall magnitude of the model forecast error is much larger because RAOBs were used for verification. This was done for reasons outlined in section 1. Additionally, some of the forecast skill success of the 10-km simulations is likely a function of the Grell CP scheme, which is better suited for this grid size versus the larger 36-km spacing (Grell 1993).

With respect to temperature from TAMDAR, the largest improvements were seen between AD10 and AN10. The additional σ-levels made a notable difference; however, reducing the grid size from 36 to 10 km, along with the additional σ-levels, had the largest impact. This is partially because the control (AN10) also had less error.

With respect to relative humidity from TAMDAR, the largest improvements were also seen between AD10 and AN10. This suggests that increasing the horizontal resolution is just as important, if not more important, than increasing the vertical resolution, and is consistent with the understanding that RH is extremely variable in both (x, y) as well as (z). Overall, maximum improvements from TAMDAR were found to be between 20-25% for RH and T, and around 10% for winds. Greater gains are expected for 4DVAR assimilation methods, but for consistency purposes, 3DVAR was employed in this study.

6. ACKNOWLEDGMENTS

The authors would like to thank Stan Benjamin (NOAA/ERL/FSL) for his comments and suggestions on RAOBs as a better means of verification. The authors are very grateful for the computer support provided by NCAR. We would like to acknowledge the NASA Aeronautics Research Office's Aviation Safety Program, the FAA Aviation Weather Research Program, and AirDat, LLC for their support in this effort.

7. REFERENCES

Benjamin, S. G., W. R. Moninger, T. L. Smith, B. D. Jamison, E. J. Szoke, T. W. Schlatter, 2007: 2006 TAMDAR impact experiment results for RUC humidity, temperature, and wind forecasts, AMS Annual Meeting, 11th Symp. IOAS-AOLS.

Bolton, D., 1980: The Computation of Equivalent Potential Temperature. *Mon. Wea. Rev.*, **108**, 1046-1053.

Brooks, H. E., and C. A. Doswell, 1996: A Comparison of Measures-Oriented and Distributions-Oriented Approaches to Forecast Verification. Weather and Forecasting, **11**, 288-303.

Cram, J. M., Y. Liu, S. Low-Nam, R-S. Sheu, L. Carson, C. A. Davis, T. Warner, J. F. Bowers, 2001: An operational mesoscale RT-FDDA analysis and forecasting system. Preprints 18th WAF and 14th NWP Confs., Ft. Lauderdale, AMS, Boston, MA.

Dudhia, J., 1993: A nonhydrostatic version of the Penn State / NCAR mesoscale model: Validation tests and simulation of an Atlantic cyclone and cold front. *Mon. Wea. Rev*., **121**,1493-1513.

Grell, G. A., 1993: Prognostic evaluation of assumptions used by cumulus parameterizations. *Mon. Wea. Rev.*, **121**, 764-787.

Grell, G. A., J. Dudhia, and D. R. Stauffer, 1994: A description of the Fifth-Generation Penn State/NCAR Mesoscale Model (MM5). NCAR Tech. Note NCAR/TN-398+STR,122 pp.

Jacobs, N. A., and Y. Liu, 2006: A Comprehensive Quantitative Precipitation Forecast Statistical Verification Study, Documentation and Tech. Note AirDat, LLC, 25 pp.

Jacobs, N. A, Y. Liu, and C.-M. Druse, 2006: Evaluation of temporal and spatial distribution of TAMDAR data in short-range mesoscale forecasts, AMS Annual Meeting, 10th Symp. IOAS-AOLS.

Jacobs, N. A, Y. Liu, and C.-M. Druse, 2007: The effects of vertical resolution on the optimization of TAMDAR data in short-range mesoscale forecasts, AMS Annual Meeting, 11th Symp. IOAS-AOLS.

Kain, J. S., and J. M. Fritsch, 1993: Convective parameterization for mesoscale models: The Kain-Fritsch scheme. The representation of cumulus convection in numerical models, K. A. Emanuel and D. J. Raymond, Eds., Amer. Meteor. Soc., 246 pp.

Kalnay, M. Kanamitsu, and W.E. Baker, 1990: Global numerical weather prediction at the National Meteorological Center. Bull. Amer. Meteor. Soc., **71**, 1410-1428.

Liu, Y., S. Low-Nam, R. Sheu, L. Carson, C. Davis, T. Warner, S. Swerdlin, J. Bowers, M. Xu, H-M Hsu, and D. Rife, 2002: Performance and Enhancement of the NCAR/ATEC mesoscale FDDA and forecast system. 15th Conference on Numerical Weather Prediction, 12-16 August, 2002, San Antonio, Taxes, 399-402.

Mahoney, K.M., and G.M. Lackmann, 2006: The sensitivity of numerical forecasts to convective parameterization: A case study of the 17 February 2004 east coast cyclone. *Wea. Forecasting*, **21**, 465–488.

Mesinger, F., G. DiMego, E. Kalnay, K. Mitchell, P.C. Shafran, W. Ebisuzajki, D. Jovic, J. Woollen, E. Rogers, E. H. Berbery, M.B. Ek, Y. Fan, R. Grumbine, W. Hyggins, H. Li, Y. Lin, G. Manikin, D. Parrish, and W. Shi, 2006: North American Regional Reanalysis, *Bulletin of the American Meteorological Society*, **87**: 343-360.

Stauffer, D. R., and N. L. Seaman, 1994: Multiscale four-dimensional data assimilation. J. Appl. Meteor., **33**, 416-434.

Xie, Y. F., C. Lu, and G. L. Browning. 2002. Impact of formulation of cost function and constraints on three-dimensional variational data assimilation. *Mon. Wea. Rev.* **130**, no. 10: 2433-47.